HAL
open science

Yttrium and Rare Earth Elements partitioning in seawaters from the Bay of Bengal.

Zhaojie Yu, Christophe Colin, Éric Douville, L. Meynadier, S. Duchamp-Alphonse, S. Sepulcre, S. Wan, L. Song, Qiong Wu, Zhaokai Xu, et al.

To cite this version:

Zhaojie Yu, Christophe Colin, Éric Douville, L. Meynadier, S. Duchamp-Alphonse, et al.. Yttrium and Rare Earth Elements partitioning in seawaters from the Bay of Bengal.. Geochemistry, Geophysics, Geosystems, 2017, 18 (4), pp.1388-1403. 10.1002/2016GC006749 . hal-01511154

HAL Id: hal-01511154

https://hal.science/hal-01511154v1

Submitted on 12 Oct 2020

HAL is a multi-disciplinary open access archive for the deposit and dissemination of scientific research documents, whether they are published or not. The documents may come from teaching and research institutions in France or abroad, or from public or private research centers.

L'archive ouverte pluridisciplinaire **HAL**, est destinée au dépôt et à la diffusion de documents scientifiques de niveau recherche, publiés ou non, émanant des établissements d'enseignement et de recherche français ou étrangers, des laboratoires publics ou privés.

AGU PUBLICATIONS

Geochemistry, Geophysics, Geosystems

RESEARCH ARTICLE

10.1002/2016GC006749

Key Points:
- First spatial distribution of dissolved REE concentrations in the BoB
- Y/Ho, Sm/La, and MREE/MREE* ratios were used to discriminate the sources of REE and scavenging or remineralization processes in the BoB
- G-B river inputs contribute significantly to the global REE budget and could largely compress the residence time of REE in the BoB

Supporting Information:
- Supporting Information S1

Correspondence to:
Z. Yu,
yuzhj1988@gmail.com

Citation:
Yu, Z., et al. (2017), Yttrium and rare earth element partitioning in seawaters from the Bay of Bengal, *Geochem. Geophys. Geosyst.*, *18*, 1388–1403, doi:10.1002/2016GC006749.

Received 23 NOV 2016
Accepted 15 MAR 2017
Accepted article online 17 MAR 2017
Published online 6 APR 2017

© 2017. American Geophysical Union. All Rights Reserved.

Yttrium and rare earth element partitioning in seawaters from the Bay of Bengal

Zhaojie Yu[1], Christophe Colin[1], Eric Douville[2], Laure Meynadier[3], Stéphanie Duchamp-Alphonse[1], Sophie Sepulcre[1], Shiming Wan[4,5], Lina Song[6], Qiong Wu[7], Zhaokai Xu[4], and Frank Bassinot[2]

[1]Laboratoire GEOsciences Paris-Sud, UMR 8148, CNRS-Université de Paris-Sud, Université Paris-Saclay, Orsay, France, [2]Laboratoire des Sciences du Climat et de l'Environnement, LSCE/IPSL, CEA-CNRS-UVSQ, Université Paris-Saclay, Gif-sur-Yvette, France, [3]Equipe de Géochimie et Cosmochimie, Institut de Physique du Globe de Paris-Sorbonne Paris Cité, UMR 7154, Université Paris Diderot, Paris, France, [4]Key Laboratory of Marine Geology and Environment, Institute of Oceanology, Chinese Academy of Sciences, Qingdao, China, [5]Laboratory for Marine Geology, Qingdao National Laboratory for Marine Science and Technology, Qingdao, China, [6]Key Laboratory of Ocean Circulation and Waves, Institute of Oceanology, Chinese Academy of Sciences, Qingdao, China, [7]State Key Laboratory of Marine Geology, Tongji University, Shanghai, China

Abstract The dissolved yttrium (Y) and rare earth element (REE) concentrations of seawater samples collected along a north-south hydrological transect within the Bay of Bengal (BoB) have been analyzed to estimate contributions of the Ganges and Brahmaputra (G-B) river inputs to the dissolved REE distribution of the Northern Indian Ocean. Surface water masses of the BoB are characterized by Y/Ho ratios (84) intermediate between the G-B river suspended sediment (41) and water mass from the South Indian Ocean (93). Covariation of MREE (middle REE, Sm) and LREE (light REE, La) concentrations suggests that the dissolved REEs in surface waters (upper 100 m depth) of the BoB (Sm/La = 0.21) appear to derive mainly from the freshwater discharge of the G-B river system. In contrast, values obtained in the intermediate and deep waters (Sm/La = 0.14) suggest a mixing of dissolved REEs deriving from the release of G-B river suspended particles (Sm/La = 0.16) and the contribution of Antarctic Bottom Water (AABW) (Sm/La = 0.12). Consequently, we propose that MREE/MREE* ratios in the BoB waters could be an accurate proxy to trace lithogenic inputs from the G-B river system. The dissolved and particle remineralization Nd fluxes from G-B river system are calculated to constitute about 9% and 4% of the global dissolved river discharge and "boundary inputs" flux. Our estimation indicates that the massive G-B river system inputs could greatly alter the dissolved REEs distribution in the BoB and contribute to the dissolved REEs budget in the ocean.

1. Introduction

In the ocean, dissolved rare earth elements (REEs) derive from continental inputs, mainly through river discharge, dissolution/scavenging of lithogenic particles transported by rivers and winds, and "boundary exchange" with continental margin sediments [*Arsouze et al.*, 2009; *Elderfield et al.*, 1988; *Frank*, 2002; *Jeandel et al.*, 2007; *Lacan and Jeandel*, 2005; *Piepgras et al.*, 1979; *Tachikawa et al.*, 2003]. Over the past decades, numerous studies have been conducted in the marginal seas or nearby major river mouths, such as the Andaman Sea [*Nozaki and Alibo*, 2003], the Bay of Bengal (BoB) [*Nozaki and Alibo*, 2003], the South China Sea [*Alibo and Nozaki*, 2000], the Sulu Sea [*Nozaki et al.*, 1999], the Caribbean Sea [*Osborne et al.*, 2015], and the Amazon estuary [*Rousseau et al.*, 2015], in order to constrain the potential factors that influence the spatial distribution of dissolved REE concentrations in modern seawater. Most of these studies highlight the fact that the spatial distribution of dissolved REEs in such areas is greatly modified by river sediment discharge that originate from continental weathering and erosion. Estimation of Nd budget in the ocean also suggests that lithogenic input plays a key role in supplying Nd to the modern ocean [*Arsouze et al.*, 2009; *Tachikawa et al.*, 2003]. Thus, understanding dissolved and particulate river inputs of dissolved REEs to the ocean is important as the dissolved REE, and more specifically the Nd isotopic compositions are widely used as tracers of modern and past ocean circulation [*Colin et al.*, 2010; *Frank*, 2002; *Goldstein and Hemming*, 2003; *Haley et al.*, 2005; *Jeandel*, 1993; *Liu et al.*, 2015; *Osborne et al.*, 2015].

Previous studies have revealed that the dissolved and particulate river discharge to the ocean have distinct behaviors as regards to the potential dissolved REE sources [*Jeandel et al*., 2007; *Sholkovitz and Szymczak*, 2000]. As suggested by earlier Nd budget studies, around 70% of the river's dissolved REE load is removed from seawaters through coagulation processes of river colloidal matter in low salinity estuaries [*Elderfield et al*., 1990; *Rousseau et al*., 2015; *Sholkovitz*, 1993]. Hence, the impact of river-dissolved REE load on the dissolved REE distribution in the ocean has long been thought to be negligible compared to that of river sediment discharge [*Jeandel and Oelkers*, 2015; *Sholkovitz and Szymczak*, 2000]. However, for rivers with considerable dissolved REE flux, the dissolved REE load may have a stronger influence on the dissolved REE budget, especially in ocean surface water close to river mouths, even if almost 70% is thought to be trapped in the estuaries [*Alibo and Nozaki*, 2000; *Osborne et al*., 2015; *Rousseau et al*., 2015; *Sholkovitz*, 1993]. The Ganges-Brahmaputra (G-B) river system is considered to be the dominant terrigenous supplier to the BoB as its water and particulate matter discharge is of an order of magnitude higher than the peninsular rivers (the Mahanadi, Godavari, Krishna, and Kaveri) [*Unger et al*., 2003]. This suggests that the influence of river-dissolved load on surface water REE concentration could be significantly higher than previously thought [*Amakawa et al*., 2000; *Nozaki and Alibo*, 2003]. However, the contribution of dissolved river load to the oceanic REE distribution of the BoB has not been investigated in detail yet.

The processes of Nd exchange between river lithogenic particles and seawater have been highlighted in several previous studies [*Byrne and Kim*, 1990; *Sholkovitz et al*., 1994]. These processes include particle release and particle scavenging in the water column from the surface down to the bottom [*Byrne and Kim*, 1990; *Hathorne et al*., 2015; *Jeandel et al*., 1995]. In the BoB, it appears that the massive sediment discharge of the G-B river (1.1×10^9 t/yr) could significantly alter the dissolved REE distribution [*Nozaki and Alibo*, 2003] and the Nd isotopic composition (εNd) [*Singh et al*., 2012] in the water column through mineral/water exchange processes or dissolution occurring during the sinking of lithogenic particles. Furthermore, *Rousseau et al*. [2015] have recently documented a rapid (3 weeks) and significant release of Nd from suspended lithogenic particles in the mid and high salinity areas of the Amazon estuary, underlining the fact that river suspended particles contribute significantly to the global marine dissolved REE budget. Moreover, it has also been suggested that bottom sedimentary release and subsequent vertical diffusion is also a potential dissolved REE source to the ocean [*Elderfield and Sholkovitz*, 1987; *Haley et al*., 2004; *Lacan and Jeandel*, 2005]. Based on pore fluid, dissolved REE concentrations in near-surface sediments retrieved from the continental margin off Oregon and California (USA), *Abbott et al*. [2015] showed that HREE enrichment of pore fluids at deep slope sites is similar to the HREE enrichment of seawater. In addition, estimation of the diffusive flux of Nd out of the sediment pore fluids as well as previously published data can account for the missing Nd source flux (76×10^6 mol/yr) in global budgets as modeled by *Arsouze et al*. [2009].

While it is hypothesized that the potential processes of dissolved river load, suspended particles and bottom sediment release govern the seawater dissolved REE distribution, their relative importance has not been assessed in the specific case of the BoB where the G-B river system is characterized by one of the highest sediment discharges and freshwater fluxes in the world [*Milliman and Meade*, 1983; *Sengupta et al*., 2006]. Only one previous study reported dissolved REE concentrations in seawater of the southern BoB (station PA-9) [*Nozaki and Alibo*, 2003]. This study highlighted a key role of river suspended particles in dominating the observed dissolved REE concentrations, while bottom regeneration of dissolved REEs was ruled out based on the absence of excess ^{228}Ra in the deep waters [*Moore and Santschi*, 1986; *Nozaki and Alibo*, 2003]. However, the spatial distribution of dissolved REEs in seawater of the BoB needs to be further documented in order to better understand the role of the G-B river system in regulating the REE distribution [*Singh et al*., 2012].

Here we have investigated the dissolved Y and REE concentrations of seawater samples collected at six stations along a 89°E meridian north-south oceanographic transect within the BoB, in order to (i) establish the spatial distributions of dissolved REE concentrations and PAAS-normalized REE patterns; (ii) assess the relative significance of dissolved river load, suspended particles, and bottom sediments release in explaining the dissolved REE distribution; and finally (iii) estimate the potential important REE flux from G-B river and its influence on the residence time of dissolved REEs in the BoB.

2. Hydrological Setting

The BoB is mainly fed in the north by the G-B river system [*Curray and Moore*, 1971] and, to a lesser extent, by rivers from the Indo-Burman ranges in the east, the Irrawaddy River (freshwater discharge: 0.4×10^{12}

m^3/yr; sediments discharge: 2.3–3.3 $\times$ 10^8 t/yr) [*Robinson et al*., 2007] and in the west by several Indian peninsular rivers (total freshwater discharge: 0.2 $\times$ 10^{12} m^3/yr; total sediment discharges: 2.4 $\times$ 10^8 t/yr) [*Tripathy et al*., 2011]. Ninety percent of the annual G-B river sediments are transferred during the summer monsoon rainfall (July–September) [*Shetye et al*., 1996; *Wyrtki*, 1973]. Associated with the summer rainfall, the G-B river contributes about 1.1 $\times$ 10^9 t/yr of sediment, and 1 $\times$ 10^{12} m^3/yr of freshwater discharge respectively to the BoB: these dominate the river input budget to the BoB [*Milliman and Meade*, 1983; *Sarin and Krishnaswami*, 1984; *Sengupta et al*., 2006]. Due to large freshwater influx during the wet summer monsoon, a plume of sea surface salinity reduction ($\sim$7‰) can be observed up to 15°N of latitude in the BoB [*Levitus et al*., 1994].

The surface circulation of the BoB is characterized by a semiannual reversal driven by the Indian monsoon. Surface water masses in the BoB (upper 100 m) include the Eastern Indian Ocean surface water, Arabian Sea high salinity water in the south and the BoB less saline surface water in the north (Figure 1). The intermediate waters (100–1500 m) are dominated by the BoB subsurface water, North Indian Intermediate Water and North Indian Deep Water [*Shankar et al*., 2002; *Wyrtki*, 1973]. Below 2000 m, the bottom waters of the BoB are largely dominated by the Antarctic Bottom Water (AABW) [*Singh et al*., 2012].

3. Materials and Methods

Eighty-six seawater samples were collected at six stations (MONO01, 02, 03, 4b, 06, and 09) in the BoB, from $\sim$17°N to $\sim$8°N, during the R/V Marion Dufresne MONOPOL Cruise in June 2012, i.e., at the beginning of the summer monsoon (Figure 1). These seawater samples were collected using 15 L, Teflon-lined, Niskin bottles which were mounted on a conductivity, temperature, and depth (CTD) profiler (Sea-Bird 911 plus, Sea-Bird Electronics Inc.) equipped with a transmissivity-sensor. All of the seawater samples were filtered on board using AcroPak 500 capsule filters (0.45 μm) and acidified to a pH lower than 2 with suprapur 6 N HCl acid immediately after sampling following GEOTRACES recommendations [*van de Flierdt et al*., 2012].

Dissolved REE concentrations were measured using the Inductively Coupled Plasma-Quadrupole Mass Spectrometer (ICP-MS X Series^{II} Thermo Fisher) at the Laboratoire des Sciences du Climat et de l'Environnement (LSCE) in Gif-sur-Yvette, France, following the method from *Wu et al*. [2015]. Briefly, an ultra-pure $FeCl_3$ solution and a spike solution enriched in Pr and Tm were then added to each sample ($\sim$250 mL) with contents around 10–70 fold higher than REE concentration in samples. After 48 h of equilibration, the pH was adjusted to $\sim$8, using ultraclean NH_4OH leading to the formation of iron hydroxides, which in turn, efficiently scavenge REEs out of the seawater samples. The REE coprecipitated fractions were separated from the remaining solution through several centrifugations and careful rinsing with Milli-Q water. The residues were then redissolved by adding 3 N HNO_3 and evaporated to dryness. The dried samples were redissolved in 2 mL 8 N HNO_3 and 50 μL of HF to remove any possible hydrated silica residues precipitated during the Fe coprecipitation step. After drying, REEs were separated from the matrix through anion exchange columns (AG1-X8 resin, mesh 100–200).

The added Pr and Tm spikes allowed the calculation of the REE extraction step recovery and finally REE concentrations in taking into account the initial Pr and Tm content in seawater samples. Such calculations considered the natural molar Pr/Nd and Tm $\times$ 2/(Er + Yb) ratios of 0.22 and 0.15, respectively, typical values of seawaters from BoB and Andaman Sea [*Nozaki and Alibo*, 2003]. Analytical uncertainties associated with such regional REE ratios are low compared to uncertainties associated with ICP-QMS analysis. The recovery rate for the BoB seawater samples ranged from 60 to 100% and the REE concentrations calculated from Pr or Tm spikes revealed no notable HREE/LREE fractioning during steps of chemical extraction or ICP-QMS analysis and, for each sample, mean REE concentrations discussed here are the average of concentrations deduced from both Pr and Tm with standard deviation between the two calculations quasi-systemically lower than $<$4%. Internal REE standard and BCR-1 standard solutions were analyzed to monitor instrument drift. Due to isobaric interferences, Eu concentrations were corrected for the residual presence of Ba-generating oxides at masses 151 and 153, and Gd concentrations (measured at masse 160 which is not impacted by Pr oxides), taking into account the isobaric interference due to Dy presence (2.34%). Calibration curves for determination of REE concentrations were validated by analysis of two geological standards BCR-1 and GRS-6 prepared at various dilutions with gaps systematically lower than 3% with BCR-1. Blank contributions are considered negligible for all REE since analysis of chemical blanks (spike solutions before and after chemistry) revealed REE signal systematically lower than 1% (most often less than 1‰) compared

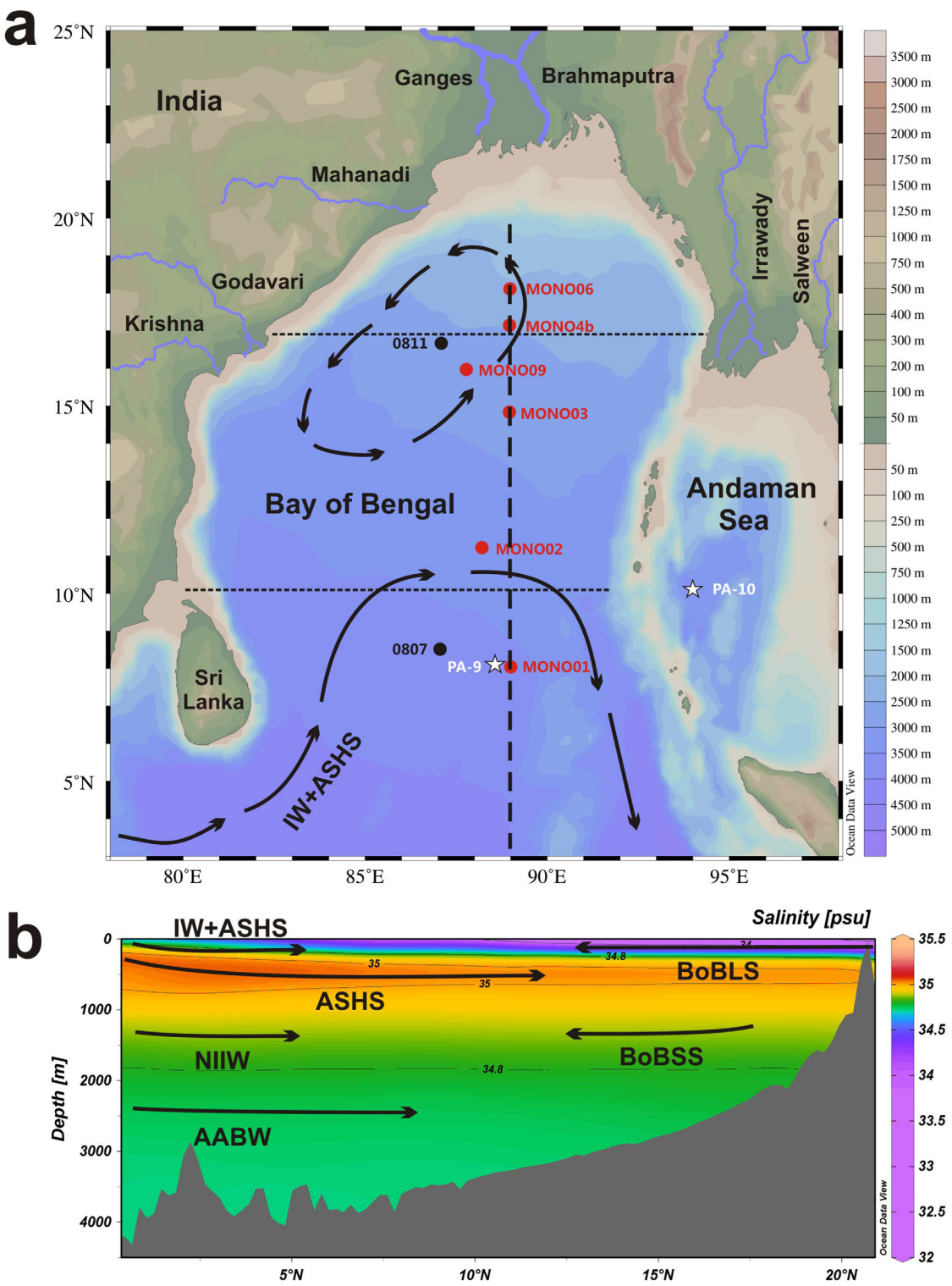

Figure 1. (a) Locations of sampling sites (red dots) in the BoB. The locations of 0807 and 0811 in the central and southern BoB are marked by black dots [*Singh et al.*, 2012]. The white star represents the sampling location of station PA-9 [*Nozaki and Alibo*, 2003]. The black arrows indicate the general surface circulation pattern in the BoB during boreal summer (June–September) [*Shankar et al.*, 2002; *Varkey et al.*, 1996]. The black dashed line shows the 89°E transect in the BoB. (b) The salinity contours along the 89°E transect in the BoB. The salinity data were taken from the World Ocean Atlas 2013 [*Zweng et al.*, 2013].The black arrows mark the general water masses in the BoB during boreal summer (June–September), including the Eastern Indian Ocean surface water (IW), Arabian Sea high salinity water (ASHS), the BoB less saline surface water (BoBLS), the BoB subsurface water (BoBSS), North Indian Intermediate Water (NIIW), and the Antarctic Bottom Water (AABW) [*Shankar et al.*, 2002; *Singh et al.*, 2012; *Wyrtki*, 1973]. All the color contours (bathymetry) in this and subsequent figures are plotted with the help of ODV4 software [*Schlitzer*, 2015].

to REE signal obtained for each sample. Finally, our measurements were characterized by analytical uncertainties systematically below 10% (2 sigma) for all REE. Such uncertainties integrate the accuracy of calibrations (less than 3%), the addition of spike solution and its measurement (less than 2%), and finally the reproducibility. We duplicate 23 samples which were analyzed twice at various dilutions (per 3 and 20) and in two distinct sequences (supporting information Table S2).

Our reproducibility uncertainty is similar to that reported in station PA-9 (<4%) [*Nozaki and Alibo*, 2003]. The surface sample concentrations of stations MONO01 and PA-9 were also compared as those two stations are closer (supporting information Figure S1) and no large differences have been observed, suggesting a precise measurement of REE concentration in our MONO stations.

4. Results

For all the MONOPOL stations, the dissolved REE concentrations of surface water (upper 100 m) are systematically higher than values for the intermediate layers (Figure 2). This pattern is accompanied by a sharp

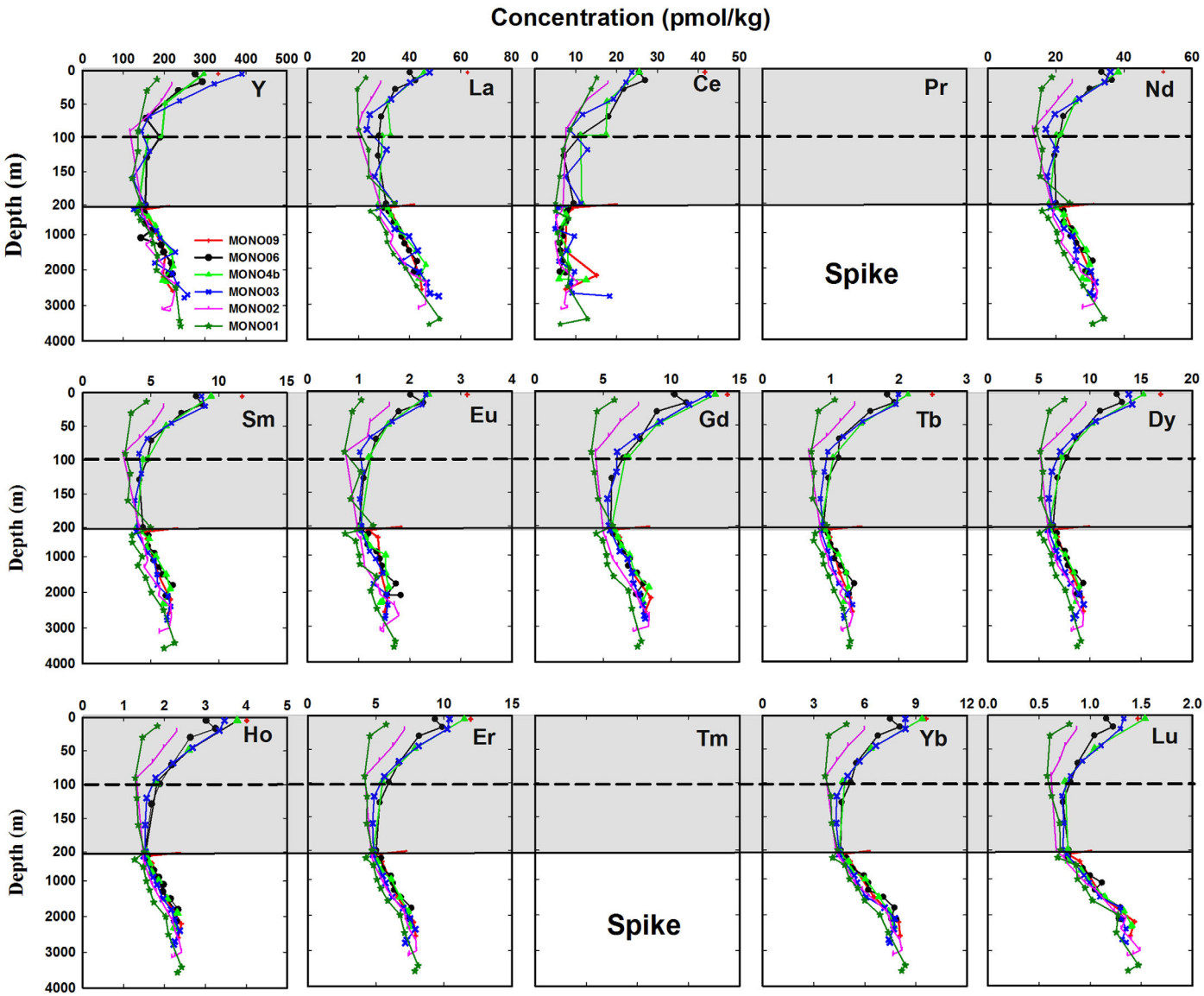

Figure 2. The concentration-depth profiles of dissolved Y and REEs in the BoB along the 89°E transect. Note that a break is made at 200 m depth and the minimum concentrations around 100 m below the surface are highlighted by dashed lines. The dissolved Pr and Tm concentrations were not measured because of the presence of the spike. The original data are shown in supporting information Table S1.

decrease of the dissolved Y and REE concentrations with depth, leading to minimum values at about 100 m depth. For example, La concentrations vary between 23 and 63 pmol/kg (mean value of 40 pmol/kg) in the upper 30 m depth and decrease to 20–30 pmol/kg (mean value of 25 pmol/kg) at a depth of 100 m.

Dissolved Y and REE concentrations in the surface water are rather scattered, which contrasts with those of intermediate and deepwater masses. This is particularly clear for stations MONO01 and 02 in the southern BoB, which display lower surface water dissolved Y and REE concentrations than the other stations (MONO03, 4b, 06, and 09) in the northern and central BoB. The surface seawater sample from station MONO09 in the central BoB shows significantly higher dissolved REE concentrations than the other stations (e.g., La concentration in the surface seawater of MONO09 is 63 pmol/kg, whereas the MONO03 and 4b surface seawater samples are about 48 pmol/kg).

Below 100 m of water depth, Y and REE concentrations of all MONOPOL stations (with the exception of Ce) increase downward with depth (e.g., La concentrations below 100 m water depth range from 20 to 52 pmol/kg, around a mean of 36 pmol/kg) (Figure 2). The dissolved REE concentrations in the intermediate and deep waters of MONOPOL stations are relatively homogenous and show an increase linearly with depth. Interestingly, the bottom water LREE (La, Ce, and Nd) and HREE (Ho, Er, Yb, and Lu) concentrations reach values that are approximately similar to those measured in surface waters, whereas MREEs (Sm, Eu, Gd, Tb, and Dy) display slightly lower concentrations. It is noteworthy that a slight decrease of the REE concentrations can be observed for the deepest samples within the water column (at about 20–30 m above the seafloor). This is particularly well marked for stations MONO01 and MONO02. The distribution of Ce concentrations in the BoB is quite different from the other REEs (Figure 2). Surface water Ce concentrations range from 15 to 28 pmol/kg (mean of 20 pmol/kg) and remain relatively low (around a mean of 10 pmol/kg) and stable below 100 m of water depth.

All of the PAAS-normalized REE patterns are quite similar and present pronounced negative Ce-anomalies as well as the progressive enrichment in MREEs and HREEs relative to LREEs (Figure 3). It is worth noting that PAAS-normalized dissolved REE pattern of surface water from station PA-9 [*Nozaki and Alibo*, 2003] agrees well with those of MONO01 since their sampling locations are very close together (Figures 1a, 4a and SOM Figure 1). In detail, the surface seawater samples display distinct PAAS-normalized REE patterns compared to intermediate and deepwater samples, with a robust enrichment in MREEs and HREEs particularly well observed for the northern and central stations MONO09, 06, 4b, and 03. This is particularly well observed in the linear plot of PAAS-normalized dissolved REE patterns for sea surface water samples that shows an enrichment from Eu to Yb with a peak at Er, which is not observed in deep water samples (Figure 3a).

5. Discussion

5.1. Sources and Significance of the Dissolved REE Distribution in the BoB

Dissolved REE concentrations depth profiles of the BoB typically show a relatively high values in surface waters, a minimum in the shallow subsurface (around 100 m), followed by a gradual increase with depth. This is associated with distinct patterns in MREEs suggesting different sources for the dissolved REEs of surface and deepwater masses in the BoB.

5.1.1. Surface Water

The possible sources of dissolved REE in the surface water include river drainage from the Indian continent (dissolved REEs in freshwater river discharge and river suspended particles), dust input to the BoB, and mixing of Arabian Sea Water and Eastern Indian Ocean Water. During the Indian summer monsoon, southwesterly winds begin to blow over most of the North Indian Ocean: these winds can drive the Arabian Sea surface water and/or Eastern Indian Ocean Water into the BoB and even into the Andaman Sea [*Shankar et al*., 2002]. Consequently, the Arabian Sea and/or Eastern Indian Ocean surface waters are important sources for the BoB surface waters, at least in the southern part of the bay during the summer monsoon season. Indeed, the PAAS- and MONO01-90 m-normalized patterns of Arabian Sea [*German and Elderfield*, 1990] and Eastern Indian Ocean surface waters [*Amakawa et al*., 2000] are similar to those of the BoB (Figure 4). Moreover, the contribution of the Andaman Sea or the Indonesian Through Flow Water is probably negligible at this time, as it is prevented by the wind driven currents which predominantly flow north-eastward (Figure 1). The dissolved REE pattern of the Ganges River shows MREE-rich patterns that have also been observed in

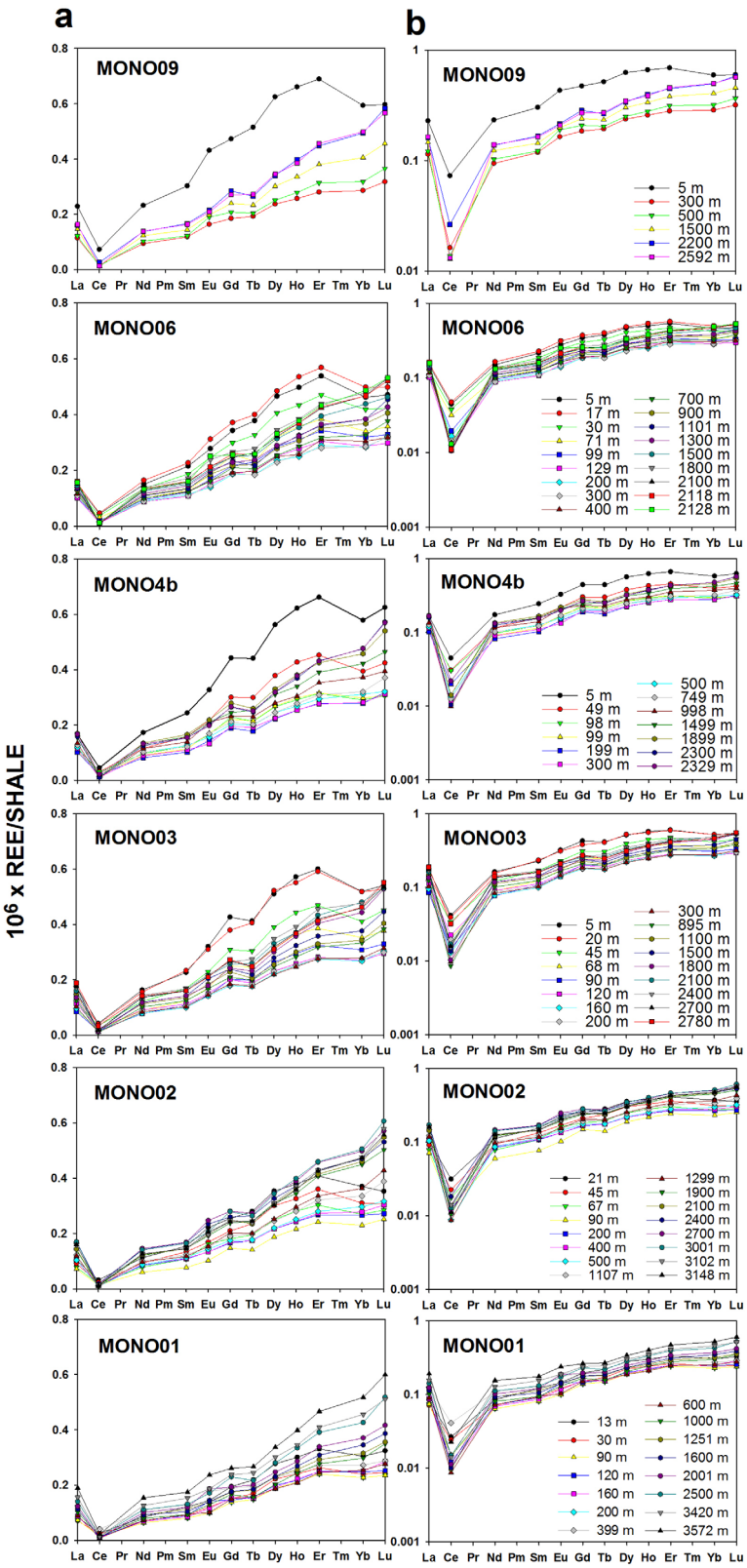

Figure 3. REE patterns for each station normalized to Post-Achaean Australian Shale (PAAS) [*Taylor and McLennan*, 1985], plotted on both (a) linear scale and (b) log scale.

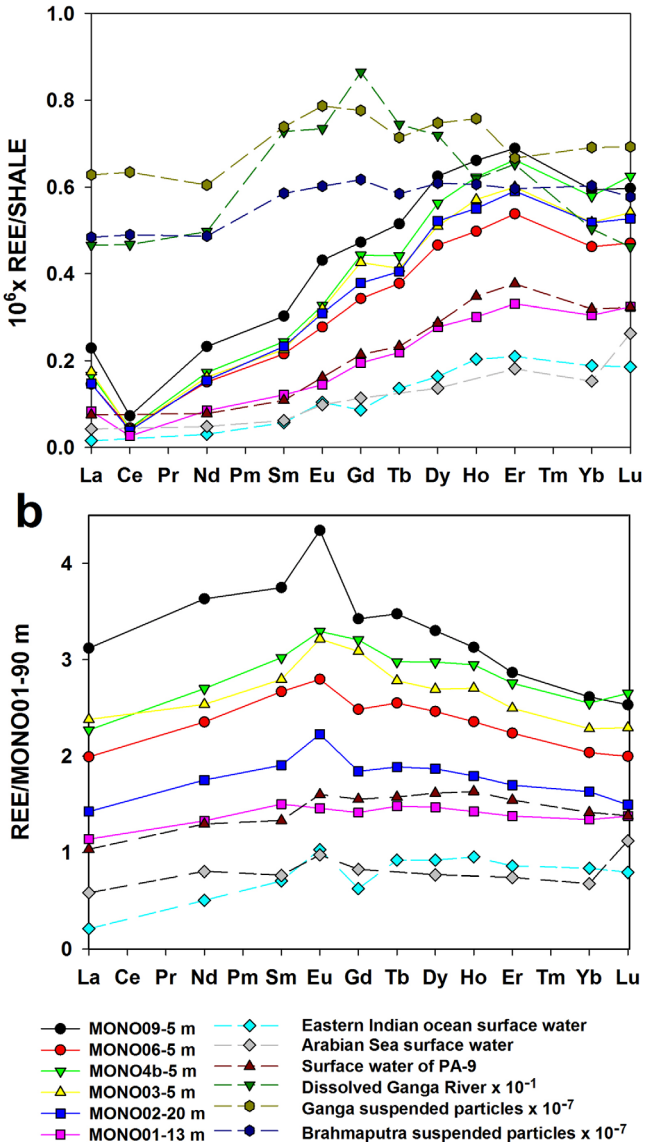

Figure 4. Surface water REE patterns. (a) PAAS-normalized [*Taylor and McLennan*, 1985] REE concentration patterns of the surface waters of MONOPOL stations in the BoB (solid line). PAAS-normalized REE concentration patterns of Eastern Indian Ocean surface water [*Amakawa et al.*, 2000], Arabian Sea surface water [*German and Elderfield*, 1990], surface water from station PA-9 in the BoB [*Nozaki and Alibo*, 2003], dissolved Ganges River water [*Rengarajan and Sarin*, 2004], and suspended particles of the G-B system [*Garzanti et al.*, 2011] are shown for comparison (dashed line). (b) MONO01-90 m-normalized surface water for MONOPOL stations in the BoB and its potential sources.

the seawater of the BoB (Figure 4a) [*Rengarajan and Sarin*, 2004]. Suspended particles of the G-B river system show relative enrichment of MREEs and HREEs compared to LREEs (Figure 4a) [*Garzanti et al.*, 2011].

In order to explore the influence of these additional REEs on BoB surface waters, all the REE concentrations of the sea surface samples from all MONO stations have been normalized to MONO01 at 90 m depth (the bottom sample of surface water in the southernmost station, Figure 4b). This normalization to the southernmost sample in the BoB, which displays the lowest dissolved REE concentrations, permits us to establish the distribution scheme of surface water dissolved REEs along the north-south transect relative to seawater samples treated using exactly the same analytical method. Each normalized dissolved REE profile displays a similar pattern with enrichment in MREE and peaks at Eu or Sm (Figure 4b). Interestingly, the samples collected in the northern and central part of the bay (MONO09, 06, 4b, and 03) indicate a relatively higher content of MREE than those retrieved in the southern part of the BoB (MONO02 and 01). This dichotomy may be attributed to the direct contribution of dissolved REEs from the G-B river system.

The dissolution of dust particles could also significantly change the ocean surface distribution of dissolved REEs [*Greaves et al.*, 1994; *Tachikawa et al.*, 1999]. The major dust source regions to the BoB are Chinese loess and alluvial dusts from the Indo-Gangetic Plain [*Kumar et al.*, 2010], which are delivered in large quantities to the bay, resulting in deposition of about 0.3–6 g/m^2/yr of mineral dust [*Srinivas and Sarin*, 2013]. This estimation is far less compared to the terrigenous flux of the northern and central BoB (average 16.5 and 15.4 g/m^2/yr) but is comparable to the southern bay (5.2 g/m^2/yr) as revealed by sediment trap study in the BoB [*Unger et al.*, 2003]. In order to identify the main source of surface excess REEs and to reveal their contributions, the HREE/LREE ratio versus MREE/MREE* ratio has been reported in Figure 5. The surface waters of the BoB exhibit HREE/LREE and MREE/MREE* ratios ranging from 3 to 4 and from 1.1 to 1.4, respectively (Figure 5). Hence, neither the dissolution of suspended river particles nor Chinese loess is a major source in the surface water of the BoB. Furthermore, some of the BoB surface samples reveal MREE/MREE* $>$ 1.3, suggesting that the dissolved G-B river inputs could play a major role as MREE/MREE* values from the other potential sources are generally lower than 1.3.

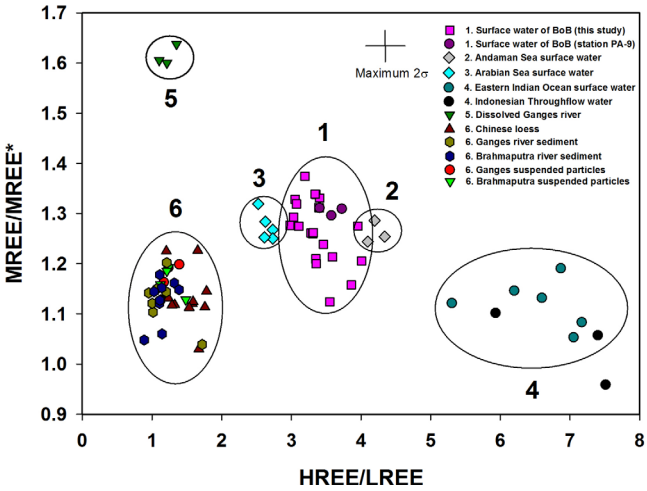

Figure 5. Surface seawater samples of the BoB and previously published values plotted as PAAS-normalized [*Taylor and McLennan*, 1985] HREE/LREE (Yb/Nd) versus MREE/MREE* (average of Gd and Dy/average of Yb and Nd). Potential sources for the BoB surface seawater are Eastern Indian Ocean surface water and Indonesian Throughflow water [*Amakawa et al*., 2000], suspended particles of G-B system [*Garzanti et al*., 2011], Arabian Sea surface water [*German and Elderfield*, 1990], Chinese loess [*Yang et al*., 2007], dissolved Ganges River water [*Rengarajan and Sarin*, 2004], and G-B river sediment [*Garzanti et al*., 2010]. Also shown for comparison is surface water from station PA-9 in the BoB and station PA-10 in the Andaman Sea [*Nozaki and Alibo*, 2003]. The error bar was estimated by the analytical uncertainties of each element.

Considering the MREE-rich influence of dissolved G-B river inputs in the surface waters of the BoB, MREE (Sm) versus LREE (La) plots may be useful for distinguishing the sources that control the REE partitioning in intermediate and deep waters (Figure 7). All results for MREE (Sm) and LREE (La) concentrations display two fitting lines, suggesting that at least a third source of REEs plays a major role in the MREE signature of seawater in the BoB (Figure 7b). Results obtained for the BoB surface water fit a first line (Sm/La = 0.21) corresponding to the mixing of dissolved G-B river inputs and the Eastern Indian Ocean surface and/or Arabian Sea high salinity waters.

Hence, the surface waters of the BoB appear here to be dominated by the mixing of dissolved G-B river inputs with southern sourced surface waters corresponding to the Eastern Indian Ocean surface water and the Arabian Sea high salinity water. This observation is particularly notable because previous studies in estuaries have suggested that up to 70% of the river-dissolved REEs are removed in the low salinity mixing regions, and that the release of dissolved REEs from sediments and resuspended particles were responsible for the subsequent increase of REE concentrations in high salinity areas [*Goldstein and Jacobsen*, 1988a; *Nozaki et al*., 2000; *Rousseau et al*., 2015; *Sholkovitz*, 1993]. The dissolved REE values from the Yamuna River are the only dissolved REE study from the G-B river system by far. This river is representative of the Ganges River as its drainage area is the largest among all the tributaries [*Rengarajan and Sarin*, 2004]. The Yamuna confluences with the Ganges at Allahabad, India, contributing about 25% of the total fresh discharge of the Ganges River [*Gupta*, 2008]. Moreover, the Yamuna River drains most of the geological formations of the southern slope of Himalaya (Higher Himalaya, Lesser Himalaya, and Siwaliks) and the Indo-Gangetic Plain, similar to most of the Ganges tributaries (Ghaghara, Gandak, Kosi, Gomti, etc.). Previous studies also indicated that those tributaries are yielding broadly consistent chemical properties in the river waters [*Galy and France-Lanord*, 1999; *Galy et al*., 1999]. Thus, we assume that the dissolved REE concentrations of Yamuna River represent those of Ganges River but further studies would be helpful to better constrain it. Nevertheless, the mean concentration of dissolved Nd in the Yamuna River (main upstream river of the Ganges River) is about 540 ± 50 pmol/kg and the total freshwater flux of G-B river is about 1×10^{12} m^3/yr [*Milliman and Meade*, 1983; *Rengarajan and Sarin*, 2004], hence, the total dissolved Nd flux into the BoB becomes 2.4×10^{-7} mol/m^2/yr as the area of the entire BoB measures 2.2×10^{12} m^2. Assuming that only 30% of the dissolved REEs passes through the estuary, the dissolved Nd input into the BoB reaches up to 0.8×10^{-7} mol/m^2/yr, comparable to the vertically integrated flux (3×10^{-7} mol/m^2/yr) previously estimated in the BoB [*Nozaki and Alibo*, 2003], implying the large contribution of dissolved G-B river inputs.

The Y and Ho concentrations of surface seawater samples have been reported in the Figure 6 in comparison with those of sediments from the G-B river system and seawater from station PA-9 and from the Southern Indian Ocean. The behavior of Y had long been recognized to match that of Ho in the ocean [*Zhang et al*., 1994]. However, the large ranges in Y/Ho ratios in the ocean (e.g., between 67 and 102 for the oxic eastern Mediterranean and between 85 and 120 for the Pacific seawater) reflect differences in complexation behavior corresponding to seawater inorganic and soft organic ligands of the surface of particulate matter [*Bau et al*., 1997; *Nozaki et al*., 1997]. With respect to this mechanism, fractionation of Y and Ho has been

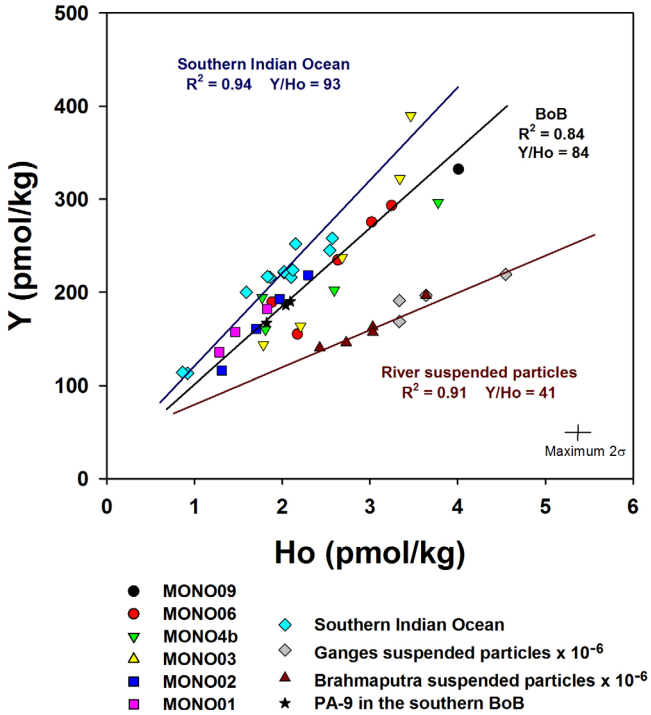

Figure 6. Surface water column profiles of Y versus Ho for MONOPOL stations in the BoB. Suspended particles from the G-B system [*Garzanti et al.*, 2011] and seawater stations IR01, IR03, and IR11 from South Indian Ocean [*Nozaki et al.*, 1997] are shown for comparison. Three straight lines represent the best fit lines for suspended particles from G-B system, BoB surface seawater, and South Indian Ocean Water, respectively. The error bar was estimated by the analytical uncertainties of each element.

attributed to the scavenging process by particulate matter rather than weathering or fluvial transport to the ocean [*Nozaki et al.*, 1997], and whether major fractionation of Y and Ho is taking place in the estuaries are still unclear [*Nozaki et al.*, 2000]. In addition, it has been estimated that Ho is scavenged about twice as fast as Y during their removal by particulate matter in the ocean [*Nozaki et al.*, 1997]. Hence, the Y/Ho ratio has been used to trace the impact of lithogenic particles on the distribution of dissolved trace elements in natural waters [*Bau et al.*, 1997]. The observed increasing trend along the particulate G-B river system (41)-seawater of the BoB (84)-South Indian Ocean (93) transect most probably highlights the intensification of sediment particle scavenging in the ocean, inducing a progressive reduction of the Ho content relative to Y in the ocean.

5.1.2. Intermediate and Deep Waters

The dissolved REE concentrations reveal a similar increasing trend with depth in the intermediate (from 100 to 2000 m in depth) and deep waters (below 2000 m, Figure 2), with concentrations higher than those observed in the open Southern Ocean [*Bertram and Elderfield*, 1993; *German et al.*, 1995]. The dissolved river flux and the wind driven mixing mainly affect the surface waters and are unlikely to impact on the water below 100 m [*Narvekar and Kumar*, 2006]. Hence, the pattern of increasing dissolved REE concentrations with depth is most probably due to the release of dissolved elements by river suspended particles during their sinking to the bottom of the ocean as also suggested by the previous study in station PA-9 [*Nozaki and Alibo*, 2003]. We cannot exclude that a part of dissolved REE enrichment at intermediate and deep depths could be associated with the release of dissolved elements through coastal/shelf sediment interactions with seawater, followed by a subsequent lateral transport of water masses from coastal to offshore regions.

It is worth noting that dissolved REE concentrations in the bottom waters of the BoB, just above the seafloor, show a slight marginal decrease (by 0.2–5 pmol/kg), in particular at stations MONO01 and MONO02. This pattern was also reported in Nd concentration studies from the central and southern BoB (Figure 1) by *Singh et al.* [2012] and at station PA-9 by *Nozaki and Alibo* [2003]. This removal of Nd could be associated with inorganic scavenging and/or kinetic balance of particle-solute interactions at the sediment-water interface [*Nozaki and Alibo*, 2003]. In any case, it demonstrates that bottom sediments are not a major REE source for bottom seawater in the BoB. Moreover, previous study in water station PA-9 also ignore this mechanism due to the lacking of ^{228}Ra in the deep waters [*Moore and Santschi*, 1986; *Nozaki and Alibo*, 2003]. Supplies of Nd to the bottom waters from sediment pore water and its upward diffusion were revealed on the continental margins off Oregon, California [*Abbott et al.*, 2015] and in the Niger Delta [*Bayon et al.*, 2011]. A direct measurement of dissolved REE concentrations in the BoB sediments pore waters are needed to further solve this issue.

Nerveless, in the diagram Sm versus La, results obtained for the intermediate and deep waters samples of the BoB fit along a second straight line (Sm/La = 0.14, Figure 7b) corresponding to the mixing of G-B river suspended particles (Sm/La = 0.16) and the AABW (Sm/La = 0.12). Such result confirms that the dissolved

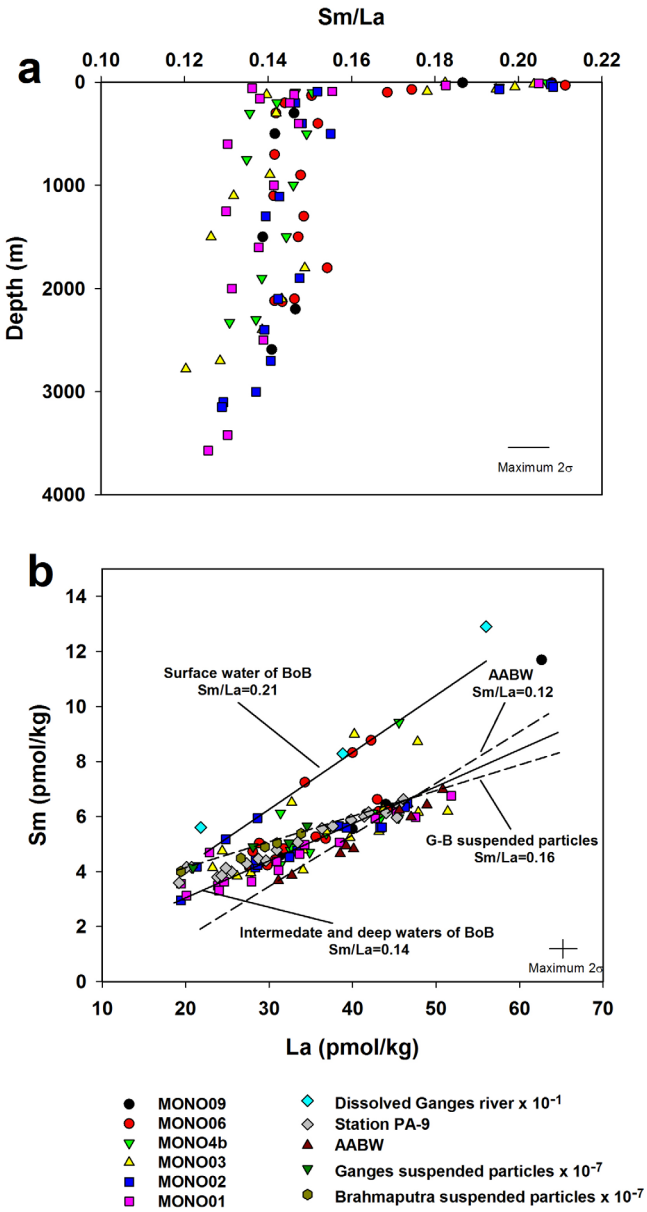

Figure 7. Water column profiles of (a) Sm/La versus depth for the MONOPOL stations in the BoB and (b) La versus Sm diagram for the MONOPOL stations in the BoB. Dissolved Ganges River water [*Rengarajan and Sarin*, 2004], station PA-9 from the BoB [*Nozaki and Alibo*, 2003], Antarctic Bottom Water (AABW) [*Bertram and Elderfield*, 1993; *German et al.*, 1995], and suspended particles from G-B system [*Garzanti et al.*, 2011] are shown for comparison. The error bar was estimated by the analytical uncertainties of each element.

REE partitioning in intermediate and deep waters are driven by a mixture of dissolution and desorption processes of G-B river suspended particles. This diagram indicates that it is possible to distinguish the dissolved REE sources of the BoB based on the MREE/LREE ratios illustrated here by the Sm/La ratio.

5.2. Influence of the G-B River Inputs on Dissolved REE Distribution in the BoB

MREE/MREE* ratios in the BoB seawaters are shown in Figure 8. For surface seawaters, values vary from 1.28 to 1.42, which are anticorrelated ($r^2 = 0.89$) with the salinity (Figure 8a). Higher MREE/MREE* ratios are associated with lower salinities and vice versa. This implies that high MREE/MREE* values in the BoB surface waters mainly reflect the freshwater dissolved REE inputs of the G-B river. The stations in the northern part of the BoB (MONO06, MONO4b, and MONO09) reveal salinity values that are generally higher than 32 psu (Figure 1). This is particularly because a strong eddy pumps high salinity subsurface water at our sampling location within the northwest part of the bay [*Murty et al.*, 1992], as was also observed for εNd anomalies (station 0811) [*Singh et al.*, 2012]. Despite the presence and influence of the eddy, linear changes of MREE/MREE* with salinity are clearly observed for surface samples and confirm a significant and direct contribution of dissolved REE rivers inputs to the dissolved REE signature of the BoB surface waters.

In addition, fractionation accompanying coagulation of river colloids occurs following the sequence of salt-induced removal as follows: LREE > MREE > HREE. This is the same succession for the release and/or scavenging of dissolved REE by suspended particles in the seawater [*Byrne and Kim*, 1990; *Elderfield et al.*, 1990; *Hoyle et al.*, 1984; *Sholkovitz*, 1993]. However, none of these processes is able to generate a MREE enrichment in seawater. Hence, the most plausible explanation for the MREE enrichment in the surface water of the BoB is a strong influence from the G-B river inputs. Therefore, in such a scenario, MREE/MREE*, which was defined as a MREE enrichment indicator, could be used as a proxy to trace the REEs that originated mainly from the G-B river inputs.

The vertical distribution of MREE/MREE* ratios displays decreasing values with increasing water depth (systematically lower than 1.1 below 500 m) (Figure 8a). Such an MREE/MREE* distribution along the water

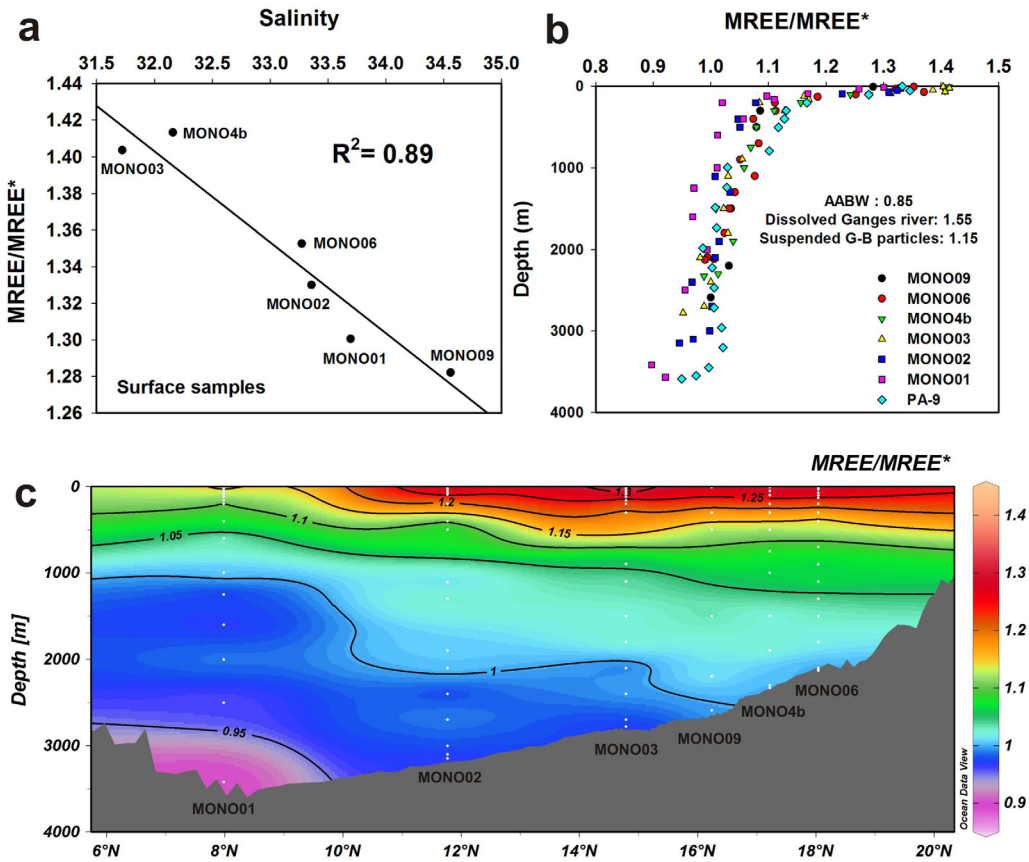

Figure 8. (a) Salinity versus MREE/MREE* in the surface water of MONOPOL stations in the BoB and (b) MREE/MREE* versus depth for MONOPOL stations and station PA-9. Note that the MREE/MREE* values of AABW [*Bertram and Elderfield*, 1993; *German et al*., 1995], dissolved Ganges River [*Rengarajan and Sarin*, 2004], and suspended G-B particles [*Garzanti et al*., 2011] are shown for comparison. (c) Distribution of MREE/MREE* in the BoB seawater stations located along the 89°E transect.

column has also been recorded at the PA-9 station [*Nozaki and Alibo*, 2003]. Analyses of dissolved REE distributions in the southeastern Atlantic Ocean and Western Indian Ocean have revealed that the MREE/MREE* value of AABW is around 0.85 [*Bertram and Elderfield*, 1993; *German et al*., 1995], whereas dissolved Ganges River and suspended G-B particles have been reported with MREE/MREE* values of around 1.55 and 1.15, respectively [*Garzanti et al*., 2011; *Rengarajan and Sarin*, 2004]. The MREE/MREE* ratios obtained in the BoB generally range between 1.55 and 0.95, implying a mixing between the end-members described above. However, the values for the surface waters are generally higher than 1.2, suggesting that the main influences are dissolved G-B river inputs that overprint the North-Western Indian Ocean signatures.

Notably, for the five stations located to the northern bay (MONO09, 06, 4b, 03, and 02), the samples collected in the upper 2000 m of water depth display MREE/MREE* values that are always greater than 1, highlighting a MREE enrichment compared to the typical value of 0.85 associated with the AABW [*Bertram and Elderfield*, 1993; *German et al*., 1995]. Furthermore, the deep water collected in the south exhibits MREE/MREE* ratios of around 0.95, which is slightly higher than those of the AABW (0.85). Such trends confirm the influence of dissolved REE desorbed from lithogenic particles in the water column. These features imply that the REE from freshwater and sediment discharges from the G-B river not only imprint the seawater column in the northern BoB but also influence the entire BoB.

5.3. Dissolved REE Flux From G-B River System and Their Residence Time in the BoB

One meaningful question here is the global significance of the sediment flux from G-B river system to the BoB and its potentially very important flux of REEs to seawater. Here Nd has been taken as an example in order to expound in detail. With the typical concentration of Nd in the suspended particles of 2.4×10^{-7} mol/g [*Garzanti et al*., 2011], the total Nd flux in the G-B riverine sediment is estimated as 2.6×10^{8} mol/yr.

For the particle-remineralization of dissolved REE in the BoB, the average lithogenic fluxes in the northern, central, and southern BoB are 16.5, 15.4, and 5.2 g/m^2/yr [*Unger et al*., 2003], average soluble particulate percentage is 15% [*Singh et al*., 2012] and hence, the suspended sediment dissolution fluxes of Nd in the northern, central and southern BoB correspond to 6.0×10^{-7}, 5.6×10^{-7}, and 1.9×10^{-7} mol/m^2/yr. This suspended sediment dissolution flux from G-B river system yields the dissolution of 1.2% of the annual sediment flux from G-B river system and is corresponding to 4% of the global "boundary exchange" flux (76×10^6 mol/yr) estimated by modeling [*Arsouze et al*., 2009]. The particle dissolution percentage (1.2%) calculated in the BoB is lower, but the same order of magnitude, than the global average value (3–5%) reported by *Arsouze et al*. [2009].

The average concentration for dissolved Nd in the Ganges River [*Rengarajan and Sarin*, 2004] is about 540 ± 50 pmol/kg, which is an order of magnitude exceeding the weighted average of 80 pmol/kg for the world's rivers [*Goldstein and Jacobsen*, 1988b]. By using this value, the total dissolved Nd flux into the BoB becomes 5.4×10^5 mol/yr (or 2.5×10^{-7} mol/m^2/yr). Assuming a subtraction of 70% of the dissolved REEs in the estuaries [*Elderfield et al*., 1990; *Rousseau et al*., 2015; *Sholkovitz*, 1993], the dissolved Nd input from G-B river system reaches up to 1.6×10^5 mol/yr (or 0.75×10^{-7} mol/m^2/yr), half order of magnitude smaller compared to the vertically integrated flux (3.0×10^5 mol/yr) calculated above. The quantity of dissolved Nd estimated from the G-B river system constitutes about 9% of the global dissolved river discharge (1.8×10^6 mol/yr) [*Arsouze et al*., 2009]. Such estimates suggest that the dissolved and solid inputs of G-B river system significantly contribute to the dissolved REE budget in the ocean.

Nozaki and Alibo [2003] used a conceptual model to simulate the reversible scavenging of dissolved REE and to calculate the residence time of dissolved REEs using the REE results from the station PA-9 in the southern BoB. The mean residence time of dissolved REEs was estimated by dividing the amount of dissolved REEs in the water column by the sum of dissolved and remineralization fluxes. They used the dissolved REE concentrations in the Chao Phraya River in Thailand as an estimate for BoB concentrations as actual dissolved REE concentrations were not available for the G-B river system at that time. Using this approach, the dissolved REE flux from the G-B river was probably underestimated. For example, the dissolved Nd concentration of the Chao Phraya River used by *Nozaki and Alibo* [2003] was 73 pmol/kg, whereas the dissolved Nd concentration from the Yamuna River reported by *Rengarajan and Sarin* [2004] was 540 ± 50 pmol/kg, almost 7 times greater than that of the Chao Phraya River. This comparison is also supported by the suspended sediment concentration calculated in the G-B river system: 1.5×10^3 mg/L, which is 1 order of magnitude higher than that of the Chao Phraya River: 0.3×10^3 mg/L [*Milliman and Meade*, 1983; *Tanabe et al*., 2003]. The riverine dissolved REE flux may be largely removed by coagulation of riverine colloids in the estuarine mixing [*Sholkovitz*, 1993]. However, it may also be rapidly released back to the seawater with the increasing of salinity in the coastal area [*Rousseau et al*., 2015; *Sholkovitz and Szymczak*, 2000]. With our dissolved REE results, it is possible to reevaluate the mean residence time of REEs and its distribution throughout the BoB.

For convenience of interpretation and discussion, we have divided the bay into three major areas: the northern BoB (north of 17°N), the central BoB (10°N–17°N), and the southern BoB (south of 10°N) (Figure 1). The dissolved REE concentrations used for each section are average values based on all seawater samples investigated in each area. Here average concentrations of Nd in northern, central, and southern BoB are 25.7, 25.2, and 21.8 pmol/kg, respectively. The mean residence time of Nd is obtained by dividing the amount of Nd in the water column by the sum of dissolved and remineralization Nd fluxes. The flux of Nd from water exchange are 1 order of magnitude smaller than the Nd inputs from sinking particles (3.0×10^6 mol) and can be neglected.

According to the partition of the three areas in the BoB, the total dissolved Nd of the northern, central and southern BoB is estimated at 5.1×10^{-5}, 7.1×10^{-5}, and 8.7×10^{-5} mol/m^2, respectively. Thus, the mean residence times of Nd with respect to the dissolved river inputs and remineralization fluxes are 61, 88, and 201 years for the northern, central, and southern BoB, respectively. The Nd residence time estimated here is clearly shorter but comparable to that of the tropical Atlantic Ocean (between 200 and 1000 years) [*Tachikawa et al*., 1999] and station PA-9 (210 years) [*Nozaki and Alibo*, 2003].

Similarly, it is possible to calculate the mean residence times for the other dissolved REEs (Table 1). The mean residence time of REEs in the BoB shows a north-south increasing trend with generally consistent and

Table 1. Estimates of Residence Times (Year) of REEs in the Bay of Bengal

Element	Northern BoB	Central BoB	Southern BoB	PA-9[a]	(Southern BoB-Northern BoB)/Northern BoB	PA-9/Southern BoB
Y	383	569	1616	1160	3.2	0.7
La	76	112	272	270	2.6	1.0
Ce	11	15	39	40	2.4	1.0
Pr	65	95	228	140	2.5	0.6
Nd	61	88	201	210	2.3	1.0
Sm	64	90	193	270	2.0	1.4
Eu	78	113	210	270	1.7	1.3
Gd	97	134	260	370	1.7	1.4
Tb	98	129	283	410	1.9	1.5
Dy	127	168	360	500	1.8	1.4
Ho	167	229	481	970	1.9	2.0
Er	194	274	580	1510	2.0	2.6
Tm	193	270	579	1390	2.0	2.4
Yb	191	285	665	1360	2.5	2.0
Lu	187	301	644	1440	2.4	2.2

[a]The residence time of PA-9 in the Bay of Bengal was reported by *Nozaki and Alibo* [2003].

shorter times in the northern and central BoB, but longer times in the southern BoB. This is especially true for HREEs. For example, the residence time of Lu is similar in northern and central BoB (187 and 301 years) but they are about 50–70% shorter (457 and 343 years) than that of southern BoB.

The estimated residence times for all dissolved REEs in the southern BoB are relatively shorter than those of station PA-9 (except for Y and Pr). These differences are smaller for LREEs but become larger for MREEs and HREEs. As the difference between calculations in our stations here in the southern part of the bay and station PA-9 is due to the higher dissolved REE concentration (Ganges River versus Chao Phraya River) and more accurate G-B river lithogenic flux (G-B river versus mean values from the Pacific) used, this reevaluation reveals that the large amounts of sediment from the G-B river could dramatically reduce the residence time of dissolved REEs in the BoB, in particular for MREEs and HREEs. This strong influence of dissolved and particulate river REE inputs observed in the BoB may be applied to the other marginal seas or nearby major river mouths that receive large river influx, e.g., Arabian Sea, South China Sea, and Caribbean Sea.

6. Conclusion

Dissolved REEs and Y concentration of six seawater stations (MONO01, 02, 03, 4b, 06, and 09) located along the 89°E meridian (from ~17°N to ~8°N) in the BoB have been investigated in order to estimate the relative importance of dissolved and lithogenic particles from the G-B river inputs, and bottom sediment releases, on the dissolved REE concentration distributions, and the residence time of dissolved REEs in the BoB. The surface dissolved REE concentrations display a decreasing trend from the surface to 100 m depth, followed by a slight downward increase below this depth. A MREE enrichment character is clearly expressed in the northern and central BoB (MONO09, 06, 4b, and 03) compared to that of the south (MONO02 and 01).

The Y/Ho ratios obtained in BoB surface seawater samples (84) are between values previously obtained in the G-B river sediments (41) and values for water masses from the South Indian Ocean (93) suggesting a north-south balance in the REE sources to the BoB. Two distinct sources of dissolved REEs are revealed based on analysis of MREE and LREE behaviors in the BoB. On the basis of the Sm (MREE) and La (LREE) covariations and Sm/La ratios, dissolved REE concentrations of the surface water of the BoB (Sm/La = 0.21) result mainly from the mixing of dissolved G-B river inputs versus the Eastern Indian Ocean surface water and/or Arabian Sea high salinity water. The Sm/La ratio in the intermediate and deep waters of the BoB (Sm/La = 0.14) is associated with mixing of another two end-members corresponding to REEs from desorption of G-B suspended lithogenic particles (Sm/La = 0.16) versus AABW contribution (Sm/La = 0.12). These two robust trends suggest that the dissolved REEs from G-B river inputs are the main source for the surface water in the BoB, whereas the release of G-B river suspended particles may largely make up the intermediate and deep waters. Furthermore, the MREE enrichment pattern in the BoB revealed here is attributed to G-B river system contributions as neither river colloid coagulation nor river particle releases tend to result in MREE enriched seawater patterns. Therefore, we proposed that MREE/MREE* ratios (particularly Sm/La) in the waters of the BoB are accurate proxies of lithogenic inputs for REEs from the G-B river system.

The dissolved Nd flux from G-B river system (1.6×10^5 mol/yr) constitutes about 9% of the global dissolved river discharge (1.8×10^6 mol/yr), while its particle remineralization flux (3.0×10^6 mol/yr) is corresponding to 4% of the total "boundary exchange" flux (76×10^6 mol/yr) estimated by the modeling. The residence times of REEs in the BoB range from 11 to 1616 years, with an overall north-south increasing trend

(170–320%). Overall, these results in the southern BoB are 1–2.6 times than those estimated in previous studies. The low residence time obtained in this study probably results from the particulate REE G-B river discharges that would largely influence the REE distribution in the BoB and their export.

Acknowledgments
The original data of this study are available in supporting information Table S1. We thank the scientific party and crew of the Marion Dufresne of MD191-MONOPOL cruise for collecting the seawater samples in the BoB. We thank the constructive comments of the two anonymous reviewers. Z. Yu acknowledges the financial support from the China Scholarship Council. We gratefully acknowledge the support provided by Louise Bordier during ICPMS analyses. We also thank Rhoda Cronin for the careful reading of the manuscript. The research leading to this study has received funding from the French National Research Agency "Investissement d'Avenir" (ANR-10-LABX-0018) and the MONOPOL project (ANR 2011 Blanc SIMI 5-6 024 04). This is LSCE contribution 6046.

References

Abbott, A. N., B. A. Haley, J. McManus, and C. E. Reimers (2015), The sedimentary flux of dissolved rare earth elements to the ocean, *Geochim. Cosmochim. Acta*, *154*, 186–200.

Alibo, D. S., and Y. Nozaki (2000), Dissolved rare earth elements in the South China Sea: Geochemical characterization of the water masses, *J. Geophys. Res.*, *105*(C12), 28,771–28,783.

Amakawa, H., D. S. Alibo, and Y. Nozaki (2000), Nd isotopic composition and REE pattern in the surface waters of the eastern Indian Ocean and its adjacent seas, *Geochim. Cosmochim. Acta*, *64*(10), 1715–1727.

Arsouze, T., J. Dutay, F. Lacan, and C. Jeandel (2009), Reconstructing the Nd oceanic cycle using a coupled dynamical-biogeochemical model, *Biogeosciences*, *6*(12), 2829–2846.

Bau, M., P. Möller, and P. Dulski (1997), Yttrium and lanthanides in eastern Mediterranean seawater and their fractionation during redox-cycling, *Mar. Chem.*, *56*(1), 123–131.

Bayon, G., D. Birot, L. Ruffine, J.-C. Caprais, E. Ponzevera, C. Bollinger, J.-P. Donval, J.-L. Charlou, M. Voisset, and S. Grimaud (2011), Evidence for intense REE scavenging at cold seeps from the Niger Delta margin, *Earth Planet. Sci. Lett.*, *312*(3), 443–452.

Bertram, C., and H. Elderfield (1993), The geochemical balance of the rare earth elements and neodymium isotopes in the oceans, *Geochim. Cosmochim. Acta*, *57*(9), 1957–1986.

Byrne, R. H., and K.-H. Kim (1990), Rare earth element scavenging in seawater, *Geochim. Cosmochim. Acta*, *54*(10), 2645–2656.

Colin, C., N. Frank, K. Copard, and E. Douville (2010), Neodymium isotopic composition of deep-sea corals from the NE Atlantic: Implications for past hydrological changes during the Holocene, *Quat. Sci. Rev.*, *29*(19), 2509–2517.

Curray, J. R., and D. G. Moore (1971), Growth of the Bengal deep-sea fan and denudation in the Himalayas, *Geol. Soc. Am. Bull.*, *82*(3), 563–572.

Elderfield, H., and E. T. Sholkovitz (1987), Rare earth elements in the pore waters of reducing nearshore sediments, *Earth Planet. Sci. Lett.*, *82*(3), 280–288.

Elderfield, H., M. Whitfield, J. Burton, M. Bacon, and P. Liss (1988), The oceanic chemistry of the rare-earth elements, *Philos. Trans. R. Soc. London A*, *325*(1583), 105–126.

Elderfield, H., R. Upstill-Goddard, and E. Sholkovitz (1990), The rare earth elements in rivers, estuaries, and coastal seas and their significance to the composition of ocean waters, *Geochim. Cosmochim. Acta*, *54*(4), 971–991.

Frank, M. (2002), Radiogenic isotopes: Tracers of past ocean circulation and erosional input, *Rev. Geophys.*, *40*(1), doi:10.1029/2000RG000094.

Galy, A., and C. France-Lanord (1999), Weathering processes in the Ganges–Brahmaputra basin and the riverine alkalinity budget, *Chem. Geol.*, *159*(1), 31–60.

Galy, A., C. France-Lanord, and L. A. Derry (1999), The strontium isotopic budget of Himalayan rivers in Nepal and Bangladesh, *Geochim. Cosmochim. Acta*, *63*(13), 1905–1925.

Garzanti, E., S. Andò, C. France-Lanord, G. Vezzoli, P. Censi, V. Galy, and Y. Najman (2010), Mineralogical and chemical variability of fluvial sediments: 1. Bedload sand (Ganga–Brahmaputra, Bangladesh), *Earth Planet. Sci. Lett.*, *299*(3), 368–381.

Garzanti, E., S. Andó, C. France-Lanord, P. Censi, P. Vignola, V. Galy, and M. Lupker (2011), Mineralogical and chemical variability of fluvial sediments: 2. Suspended-load silt (Ganga–Brahmaputra, Bangladesh), *Earth Planet. Sci. Lett.*, *302*(1), 107–120.

German, C., T. Masuzawa, M. Greaves, H. Elderfield, and J. Edmond (1995), Dissolved rare earth elements in the Southern Ocean: Cerium oxidation and the influence of hydrography, *Geochim. Cosmochim. Acta*, *59*(8), 1551–1558.

German, C. R., and H. Elderfield (1990), Rare earth elements in the NW Indian Ocean, *Geochim. Cosmochim. Acta*, *54*(7), 1929–1940.

Goldstein, S. J., and S. B. Jacobsen (1988a), REE in the Great Whale River estuary, northwest Quebec, *Earth Planet. Sci. Lett.*, *88*(3–4), 241–252.

Goldstein, S. J., and S. B. Jacobsen (1988b), Rare earth elements in river waters, *Earth Planet. Sci. Lett.*, *89*(1), 35–47.

Goldstein, S. L., and S. R. Hemming (2003), Long-lived isotopic tracers in oceanography, paleoceanography, and ice-sheet dynamics, *Treatise Geochem.*, *6*, 453–489.

Greaves, M., P. Statham, and H. Elderfield (1994), Rare earth element mobilization from marine atmospheric dust into seawater, *Mar. Chem.*, *46*(3), 255–260.

Gupta, A. (2008), *Large Rivers: Geomorphology and Management*, John Wiley, Hoboken, N. J.

Haley, B. A., G. P. Klinkhammer, and J. McManus (2004), Rare earth elements in pore waters of marine sediments, *Geochim. Cosmochim. Acta*, *68*(6), 1265–1279.

Haley, B. A., G. P. Klinkhammer, and A. C. Mix (2005), Revisiting the rare earth elements in foraminiferal tests, *Earth Planet. Sci. Lett.*, *239*(1), 79–97.

Hathorne, E. C., T. Stichel, B. Brück, and M. Frank (2015), Rare earth element distribution in the Atlantic sector of the Southern Ocean: The balance between particle scavenging and vertical supply, *Mar. Chem.*, *177*, 157–171.

Hoyle, J., H. Elderfield, A. Gledhill, and M. Greaves (1984), The behaviour of the rare earth elements during mixing of river and sea waters, *Geochim. Cosmochim. Acta*, *48*(1), 143–149.

Jeandel, C. (1993), Concentration and isotopic composition of Nd in the South Atlantic Ocean, *Earth Planet. Sci. Lett.*, *117*(3), 581–591.

Jeandel, C., and E. H. Oelkers (2015), The influence of terrigenous particulate material dissolution on ocean chemistry and global element cycles, *Chem. Geol.*, *395*, 50–66.

Jeandel, C., J. Bishop, and A. Zindler (1995), Exchange of neodymium and its isotopes between seawater and small and large particles in the Sargasso Sea, *Geochim. Cosmochim. Acta*, *59*(3), 535–547.

Jeandel, C., T. Arsouze, F. Lacan, P. Techine, and J.-C. Dutay (2007), Isotopic Nd compositions and concentrations of the lithogenic inputs into the ocean: A compilation, with an emphasis on the margins, *Chem. Geol.*, *239*(1), 156–164.

Kumar, A., M. Sarin, and B. Srinivas (2010), Aerosol iron solubility over Bay of Bengal: Role of anthropogenic sources and chemical processing, *Mar. Chem.*, *121*(1), 167–175.

Lacan, F., and C. Jeandel (2005), Neodymium isotopes as a new tool for quantifying exchange fluxes at the continent–ocean interface, *Earth Planet. Sci. Lett.*, *232*(3), 245–257.

Levitus, S., R. Burgett, and T. P. Boyer (1994), *NOAA Atlas NESDIS 3*, pp. 1–99, U.S. Dep. of Commer., Washington, D. C.
Liu, Y., L. Lo, Z. Shi, K.-Y. Wei, C.-J. Chou, Y.-C. Chen, C.-K. Chuang, C.-C. Wu, H.-S. Mii, and Z. Peng (2015), Obliquity pacing of the western Pacific Intertropical Convergence Zone over the past 282,000 years, *Nat. Commun.*, *6*, 10018, doi:10.1038/ncomms10018.
Milliman, J. D., and R. H. Meade (1983), World-wide delivery of river sediment to the oceans, *J. Geol.*, *91*, 1–21.
Moore, W. S., and P. H. Santschi (1986), Ra-228 in the deep Indian Ocean, *Deep Sea Res., Part A*, *33*(1), 107–120.
Murty, V., Y. Sarma, D. Rao, and C. Murty (1992), Water characteristics, mixing and circulation in the Bay of Bengal during southwest monsoon, *J. Mar. Res.*, *50*(2), 207–228.
Narvekar, J., and S. P. Kumar (2006), Seasonal variability of the mixed layer in the central Bay of Bengal and associated changes in nutrients and chlorophyll, *Deep Sea Res., Part I*, *53*(5), 820–835.
Nozaki, Y., and D. S. Alibo (2003), Importance of vertical geochemical processes in controlling the oceanic profiles of dissolved rare earth elements in the northeastern Indian Ocean, *Earth Planet. Sci. Lett.*, *205*(3), 155–172.
Nozaki, Y., J. Zhang, and H. Amakawa (1997), The fractionation between Y and Ho in the marine environment, *Earth Planet. Sci. Lett.*, *148*(1), 329–340.
Nozaki, Y., D.-S. Alibo, H. Amakawa, T. Gamo, and H. Hasumoto (1999), Dissolved rare earth elements and hydrography in the Sulu Sea, *Geochim. Cosmochim. Acta*, *63*(15), 2171–2181.
Nozaki, Y., D. Lerche, D. S. Alibo, and A. Snidvongs (2000), The estuarine geochemistry of rare earth elements and indium in the Chao Phraya River, Thailand, *Geochim. Cosmochim. Acta*, *64*(23), 3983–3994.
Osborne, A. H., B. A. Haley, E. C. Hathorne, Y. Plancherel, and M. Frank (2015), Rare earth element distribution in Caribbean seawater: Continental inputs versus lateral transport of distinct REE compositions in subsurface water masses, *Mar. Chem.*, *177*, 172–183.
Piepgras, D. J., G. Wasserburg, and E. Dasch (1979), The isotopic composition of Nd in different ocean masses, *Earth Planet. Sci. Lett.*, *45*(2), 223–236.
Rengarajan, R., and M. Sarin (2004), Distribution of rare earth elements in the Yamuna and the Chambal rivers, India, *Geochem. J.*, *38*(6), 551–569.
Robinson, R. A. J., M. Bird, N. W. Oo, T. Hoey, M. M. Aye, D. Higgitt, X. Lu, A. Swe, T. Tun, and S. L. Win (2007), The Irrawaddy River sediment flux to the Indian Ocean: The original nineteenth-century data revisited, *J. Geol.*, *115*(6), 629–640.
Rousseau, T. C., J. E. Sonke, J. Chmeleff, P. van Beek, M. Souhaut, G. Boaventura, P. Seyler, and C. Jeandel (2015), Rapid neodymium release to marine waters from lithogenic sediments in the Amazon estuary, *Nat. Commun.*, *6*, 7592, doi:10.1038/ncomms8592.
Sarin, M., and S. Krishnaswami (1984), Major ion chemistry of the Ganga–Brahmaputra River systems, India, *312*, 538–541.
Schlitzer, R. (2015), *Ocean Data View*. odv. awi. de.
Sengupta, D., G. Bharath Raj, and S. Shenoi (2006), Surface freshwater from Bay of Bengal runoff and Indonesian Throughflow in the tropical Indian Ocean, *Geophys. Res. Lett.*, *33*, L22609, doi:10.1029/2006GL027573.
Shankar, D., P. Vinayachandran, and A. Unnikrishnan (2002), The monsoon currents in the north Indian Ocean, *Prog. Oceanogr.*, *52*(1), 63–120.
Shetye, S., A. Gouveia, D. Shankar, S. Shenoi, P. Vinayachandran, D. Sundar, G. Michael, and G. Nampoothiri (1996), Hydrography and circulation in the western Bay of Bengal during the northeast monsoon, *J. Geophys. Res.*, *101*(C6), 14,011–14,025.
Sholkovitz, E., and R. Szymczak (2000), The estuarine chemistry of rare earth elements: Comparison of the Amazon, Fly, Sepik and the Gulf of Papua systems, *Earth Planet. Sci. Lett.*, *179*(2), 299–309.
Sholkovitz, E. R. (1993), The geochemistry of rare earth elements in the Amazon River estuary, *Geochim. Cosmochim. Acta*, *57*(10), 2181–2190.
Sholkovitz, E. R., W. M. Landing, and B. L. Lewis (1994), Ocean particle chemistry: The fractionation of rare earth elements between suspended particles and seawater, *Geochim. Cosmochim. Acta*, *58*(6), 1567–1579.
Singh, S. P., S. K. Singh, V. Goswami, R. Bhushan, and V. K. Rai (2012), Spatial distribution of dissolved neodymium and εNd in the Bay of Bengal: Role of particulate matter and mixing of water masses, *Geochim. Cosmochim. Acta*, *94*, 38–56.
Srinivas, B., and M. Sarin (2013), Atmospheric dry-deposition of mineral dust and anthropogenic trace metals to the Bay of Bengal, *J. Mar. Syst.*, *126*, 56–68.
Tachikawa, K., C. Jeandel, and M. Roy-Barman (1999), A new approach to the Nd residence time in the ocean: The role of atmospheric inputs, *Earth Planet. Sci. Lett.*, *170*(4), 433–446.
Tachikawa, K., V. Athias, and C. Jeandel (2003), Neodymium budget in the modern ocean and paleo-oceanographic implications, *J. Geophys. Res.*, *108*(C8), 3254, doi:10.1029/1999JC000285.
Tanabe, S., Y. Saito, Y. Sato, Y. Suzuki, S. Sinsakul, S. Tiyapairach, and N. Chaimanee (2003), Stratigraphy and Holocene evolution of the mud-dominated Chao Phraya delta, Thailand, *Quat. Sci. Rev.*, *22*(8), 789–807.
Taylor, S. R., and S. M. McLennan (1985), *The Continental Crust: Its Composition and Evolution*, Blackwell Sci., Oxford, U. K.
Tripathy, G. R., S. K. Singh, R. Bhushan, and V. Ramaswamy (2011), Sr–Nd isotope composition of the Bay of Bengal sediments: Impact of climate on erosion in the Himalaya, *Geochem. J.*, *45*(3), 175–186.
Unger, D., V. Ittekkot, P. Schäfer, J. Tiemann, and S. Reschke (2003), Seasonality and interannual variability of particle fluxes to the deep Bay of Bengal: Influence of riverine input and oceanographic processes, *Deep Sea Res., Part II*, *50*(5), 897–923.
van de Flierdt, T., K. Pahnke, H. Amakawa, P. Andersson, C. Basak, B. Coles, C. Colin, K. Crocket, M. Frank, and N. Frank (2012), GEOTRACES intercalibration of neodymium isotopes and rare earth element concentrations in seawater and suspended particles. Part 1: Reproducibility of results for the international intercomparison, *Limnol. Oceanogr. Methods*, *10*(4), 234–251.
Varkey, M., V. Murty, and A. Suryanarayana (1996), Physical oceanography of the Bay of Bengal and Andaman Sea, *Oceanogr. Mar. Biol.*, *34*, 1–70.
Wu, Q., C. Colin, Z. Liu, E. Douville, Q. Dubois-Dauphin, and N. Frank (2015), New insights into hydrological exchange between the South China Sea and the western Pacific Ocean based on the Nd isotopic composition of seawater, *Deep Sea Res., Part II*, *122*, 25–40.
Wyrtki, K. (1973), Physical oceanography of the Indian Ocean, in *The Biology of the Indian Ocean*, pp. 18–36, Springer, Berlin.
Yang, X., Y. Liu, C. Li, Y. Song, H. Zhu, and X. Jin (2007), Rare earth elements of aeolian deposits in Northern China and their implications for determining the provenance of dust storms in Beijing, *Geomorphology*, *87*(4), 365–377.
Zhang, J., H. Amakawa, and Y. Nozaki (1994), The comparative behaviors of yttrium and lanthanides in the seawater of the North Pacific, *Geophys. Res. Lett.*, *21*(24), 2677–2680.
Zweng, M. M., et al. (2013), World Ocean Atlas 2013, volume 2: Salinity, edited by S. Levitus and A. Mishonov, in *NOAA Atlas NESDIS*, 74, 39 pp.